

Bethe-Salpeter equation for elastic nucleon-nucleon scattering

J. Fleischer

Department of Theoretical Physics, University of Bielefeld, 48 Bielefeld, Germany

J. A. Tjon

Institute for Theoretical Physics, University of Utrecht, Utrecht, The Netherlands

(Received 27 March 1979)

The Bethe-Salpeter equation for NN scattering with one-boson exchange is investigated for the case in which the pion-nucleon coupling is described by axial-vector theory. In contrast to the results with pseudoscalar coupling, good agreement with the experimental data can be obtained for all partial waves. Also, the deviations from the Blankenbecler-Sugar equation are not as large as they are for pseudoscalar coupling. In addition, cancellations between the direct and the crossed box graph with pseudoscalar πN coupling are investigated for the 3S_1 phase shift in the framework of the variational operator Padé approximation.

I. INTRODUCTION

The Bethe-Salpeter equation (BSE) for total angular momentum $J=0$ has been described in detail in Ref. 1, and its extension to $J>0$ with a complete description of the kernel was given in Ref. 2. In these papers the interaction between pions and nucleons was considered to be of pseudoscalar (P) type. It was found that only the isospin $I=1$ phase shifts for NN scattering are in fair agreement with the experimental data. The phase shifts show in general the deficiency of dropping too fast at higher energies. For the $I=0$ channels, we found with the same meson-nucleon coupling constants used to fit the $I=0$ phase shifts that the nuclear force is in general much too strong to yield agreement with the phase shifts.

These deficiencies can be ascribed to the strong $N\bar{N}\pi$ coupling in a pseudoscalar theory, and it is necessary to weaken this coupling. This can be achieved by using an axial-vector (A) coupling for the pion-nucleon vertex. It appears therefore worthwhile to investigate the axial-vector coupling in the BSE. We find that much better phase shifts can be obtained, and even the isospin $I=0$ partial waves can be described properly.

Although the introduction of the A theory gives rise to the effective weakening of the coupling of positive- and negative-energy states, an interesting question is what possible mechanism in a pure P theory results in this weakening. One possibility is the inclusion of the crossed box graph as an additional driving force. A straightforward way to do this would be to calculate the sum of the two-particle irreducible graphs and use it as the kernel in the BSE, i.e., in our case to just add the crossed box graph to the Born term of the one-boson exchanges. In practice, however, the numerical calculation of the crossed box graph on the complete

mesh of integration points for the BSE ($\sim 200 \times 200$) consumes too much computer time. A possible alternative procedure is to use the so-called operator Padé approximants (OPA). Already in Ref. 3 we have shown that this way of handling the BSE in the case of one-boson exchanges is more efficient than the standard method of iterating the BSE and summing the perturbation series for the on-shell elements by high-order Padé approximants. Beyond that the OPA's can be considered a general formal procedure to sum the full perturbation expansion so that the inclusion of the crossed box graph is performed in a natural way. The $[1/1]$ OPA can be understood as a Bethe-Salpeter equation, the kernel of which is not the sum of the irreducible parts but the $[1/1]$ OPA on the irreducible part. In order to further simplify the calculation, we consider the off-shell momenta in the OPA as variational parameters—a method which has been surprisingly successful in potential theory.^{4,5}

In this framework we calculate the 3S_1 phase shift. To justify the method as far as possible, many tests have been performed, and, in particular, it is shown extensively how the method works for A πN coupling, since in this case one also has the standard method for comparison.

In Sec. II we describe the BSE with A coupling for the $NN\pi$ vertex. We give details of the kernel and present our numerical results for the phase shifts. Section III contains an extensive description of the method of the variational operator Padé approximation, and numerical results are given for the 3S_1 - 3D_1 channel of the ladder BSE with A coupling. The case of P coupling is studied in detail in Sec. IV, where the crossed box-graph contribution is included. It is found that this gives rise to an effective weakening of the nucleon-nucleon interaction so that the P and A theories give comparable results. Finally, in Sec. V the variational OPA is

investigated for the higher partial waves, where it turns out that extremely good results can be obtained for A coupling by using only one off-shell momentum as variational parameter.

It should be mentioned at the end that the variational OPA with P interaction works well enough so that its application to a renormalizable theory of the NN interaction⁶ can be expected to yield proper phase shifts as well.

II. THE BETHE-SALPETER EQUATION WITH AXIAL-VECTOR COUPLING

The Lagrangian for axial-vector πN coupling is given by

$$\mathcal{L} = g_A \bar{\psi} \gamma_\mu \gamma_5 \vec{T} \psi \cdot \partial_\mu \vec{\phi}, \quad (1)$$

where the coupling constant g_A is chosen such that

TABLE I. Coefficients $C(i)$ for A coupling, multiplied by 4; cf. Ref. 2.

i	Singlet $L=J$	Coupled triplet $L=J \pm 1$
1	$-E_6 Q_J + 2pq Z_J$	$-E_6 Z_J + 2pq Q_J$
2	$-(E_6 - 2)Z_J$	$(E_6 - 2)Q_J$
3	$-(E_5 - 2p^2 q^2)Q_J$	$(E_5 - 2p^2 q^2)R_J$
4	$-(E_6 + 2q^2)Z_J$	$E_6 R_J - 2pq Q_J$
5	$(E_5 + 2p^2)Q_J$	$-(E_6 - 2)Q_J$
6	$E_1 S_J$	$-(E_5 - 2p^2 q^2)Z_J$
7	$4pq S_J$	$E_1 S_J$
8	$-2Z_J$	$-E_2 S_J$
9	$2Q_J$	$E_1 S_J$
10	$2(1 - q^2)S_J$	$-E_2 S_J$
11	$E_5 R_J - 2pq Q_J$	$-(E_6 + 2q^2)Q_J$
12	$-(E_5 + 2q^2)Q_J$	$(E_5 + 2p^2)Z_J$
13	$-E_6 Z_J + 2pq(E_5^2 Q_J + qp Z_J)$	$E_1 S_J$
14	$-[E(p) - E(q)]^2 + k_0^2 S_J$	$-E_1 S_J$
15	$E_2 S_J$	$(E_6 + 2q^2)Q_J$
16		$-(E_5 + 2p^2)R_J$
17	$2(1 - p^2)S_J$	$-2Q_J$
18	$-2R_J$	$2Z_J$
19	$2Q_J$	$-2S_J$
20	$2(p^2 Z_J - pq Q_J)$	$2S_J$
21	$E_6 Q_J - 2pq R_J$	$2Q_J$
22	$(E_6 - 2)R_J$	$-2R_J$
23	$(E_5 - 2p^2 q^2)Q_J$	$-(E_5 - 2)Z_J$
24	$-2(p^2 + q^2)S_J$	$-(E_6 - 2p^2 q^2)Q_J$
25		$2(p^2 Q_J - pq Z_J)$
26	$-2(pq Q_J - q^2 R_J)$	$(E_5 - 2)R_J$
27	$-E_1 S_J$	$(E_6 - 2p^2 q^2)Q_J$
28		$-2(p^2 Q_J - pq R_J)$
29	$(E_6 + 2q^2)R_J$	$-E_5 Q_J + 2pq Z_J$
30	$-(E_5 + 2p^2)Q_J$	$E_5 Q_J - 2pq R_J$
31	$-E_5 Z_J + 2pq Q_J$	
32	$(E_5 - 2)Q_J$	
33	$(E_6 - 2p^2 q^2)R_J$	
34	$[E(p) - E(q)]^2 + k_0^2 S_J$	
35	$E_2 S_J$	
36	$E_1 S_J$	
37		

the physical (on-shell) S -matrix elements are the same as for pseudoscalar coupling with $g_p^2/4\pi = 14.2$. The corresponding spin structure of the vertices (cf. Ref. 1) read

$$V^{(1)} V^{(2)} = \frac{g_A^2}{4\pi} \not{k}^{(1)} \gamma_5^{(1)} \gamma_5^{(2)} \not{k}^{(2)}, \quad (2)$$

where the four-vector k is the momentum transfer carried by the pion. The cutoff is chosen as in Refs. 1 and 2. In Ref. 2 a general form of the kernel was written down, and accordingly it is necessary only to specify some coefficients $C(i)$, $i = 1, 2, 3, \dots$. For A coupling these coefficients are given in Table I for singlet $L=J$ and coupled triplet $L=J \pm 1$, respectively.

Taking the above matrix elements for one-pion exchange, the BSE was studied with the same meson exchanges as used in the earlier papers. Since our calculations are very time consuming, no attempt was made to perform a χ^2 fit (for possible time reductions see Sec. III).

To obtain a reasonable fit to the NN phase shifts, we varied g_η , g_ϵ , g_{ρ_1} , g_{ρ_2} , g_ω , and the cutoff Λ (cf. also Ref. 1). The results shown in Figs. 1–8 were obtained with

$$\begin{aligned} g_\eta^2/4\pi &= 3.09, & g_\epsilon^2/4\pi &= 7.3, \\ g_{\rho_1}^2/4\pi &= 0.43, & g_{\rho_2} &= 6.0, \\ g_\omega^2/4\pi &= 11.0, & \Lambda^2 &= 1.8m^2, \end{aligned}$$

where m = nucleon mass.

While the S waves are reproduced very accurately with these parameters, there are some problems with the P waves. First of all, the 3P_0 and 3P_2 are too repulsive. In a χ^2 fit in terms of the

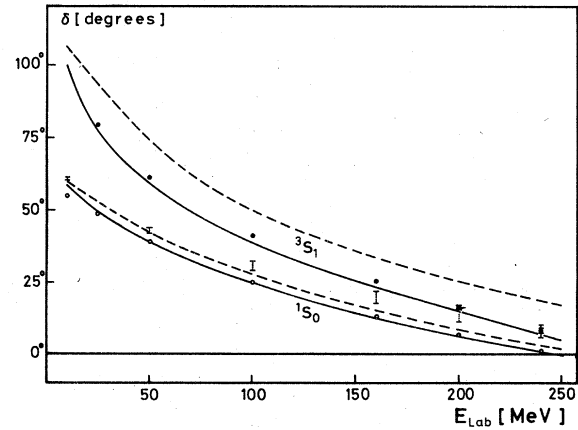
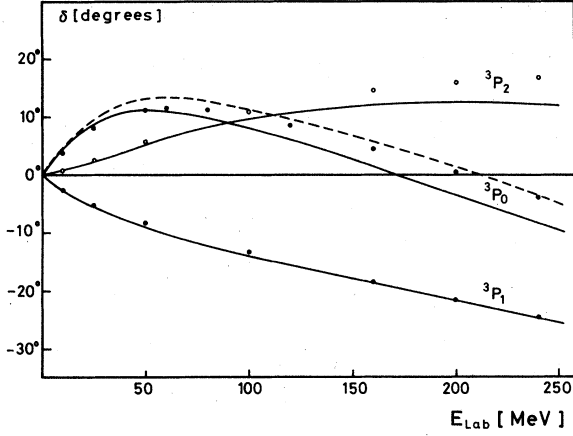


FIG. 1. 1S_0 and 3S_1 nuclear bar phase shifts. The experimental data are taken from Ref. 12, Tables IV and VI, respectively. The dashed lines are obtained from the BSE equation with the same parameters as used in the BSE.

FIG. 2. Same as Fig. 1 for 3P_0 , 3P_1 , and 3P_2 .

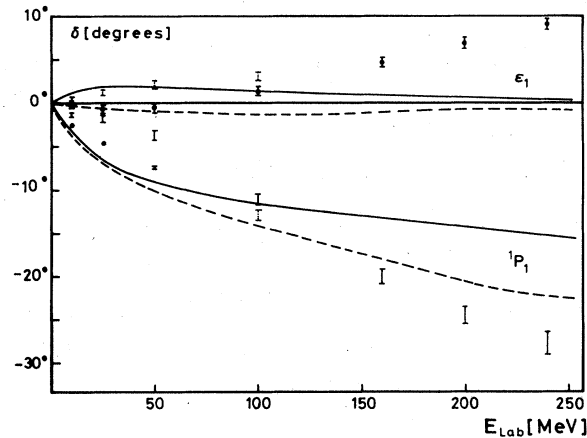
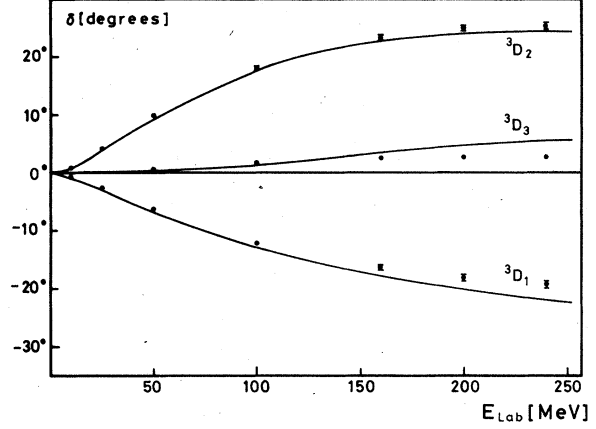
Blankenbecler-Sugar equation (BBS) by Verhoeven,⁷ these deficiencies are very nearly the same. This is not so, however, for the 1P_1 , which comes out too small in our calculation, and similarly for the ϵ_1 . Apart from these deviations from the experimental phase shifts, the overall quality of our results is comparable to that obtained in Ref. 7.

In Figs. 1, 2, and 3 we have also shown some results obtained by means of the BBS equation (dashed lines) with the same parameters as used for the BSE. With

$$g_\epsilon^2/4\pi = 7.34, \quad g_{\rho_2} = 6.8, \quad \Lambda^2 = 1.5m^2,$$

and the other parameters the same as before, the deviations from the BSE could be taken care of, except for the 1P_1 , which is nearly the same as with the above parameter set.

To conclude, we find with axial-vector πN coupling the following results: It is easier to find a good fit for the $I=1$ partial waves. It is possible to

FIG. 3. Same as Fig. 1 for ϵ_1 and 1P_1 .FIG. 4. Same as Fig. 1 for 3D_1 , 3D_2 , and 3D_3 .

obtain at the same time an acceptable fit for the $I=0$ phase shifts as well. Also, the Padé approximants converge much better. The deviations between the BSE and BBS equation are not as large as with pseudoscalar coupling (cf. Ref. 1), but they are still appreciable in some channels.

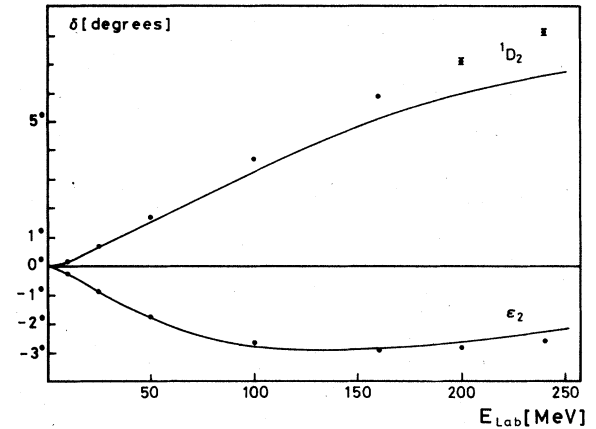
III. THE OPERATOR PADÉ APPROXIMANT

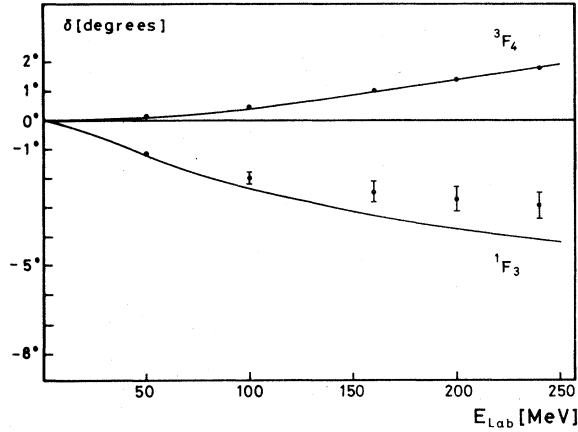
In Ref. 3 some preliminary results were presented on the applicability of operator Padé approximants^{8,9} as a method of solving the BSE for the 3S_1 phase shift with A coupling and our present parameters.

Expanding the operator K (K matrix) with respect to the strong coupling constant:

$$K = \frac{g^2}{4\pi} K_1 + \left(\frac{g^2}{4\pi}\right)^2 K_2 + \dots, \quad (3)$$

where K_1 and K_2 are operators as well, the [1/1] OPA is

FIG. 5. Same as Fig. 1 for 1D_2 and ϵ_2 .

FIG. 6. Same as Fig. 1 for 1F_3 and 3F_4 .

$$[1/1] = \frac{g^2}{4\pi} K_1 \left(K_1 - \frac{g^2}{4\pi} K_2 \right)^{-1} K_1, \quad (4)$$

which is the lowest-order approximation to the summation of the full perturbation theory in strong interactions. In particular, it solves the Bethe-Salpeter equation in ladder approximation exactly. Writing the latter as

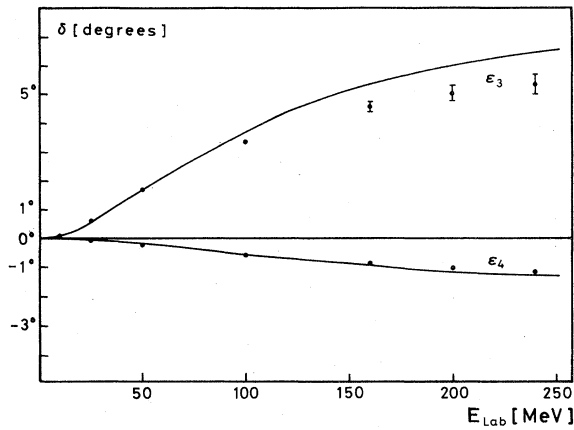
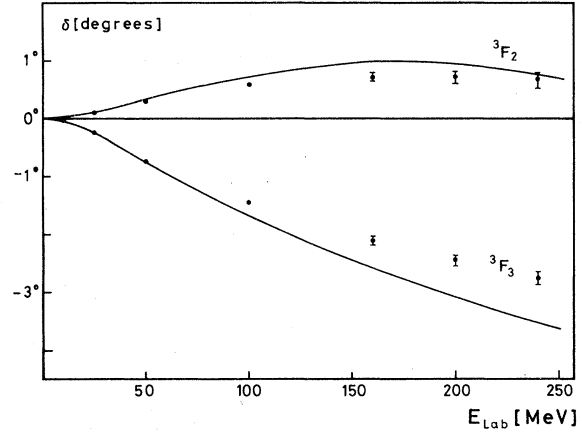
$$\phi = G + GS\phi \quad (5)$$

(G and S are the kernel and the two-nucleon propagator, respectively), it can be solved formally,

$$\phi = G(G - D)^{-1}G, \quad (6)$$

where $D = GSG$ (direct box graph), which is the $[1/1]$ OPA summation of the (geometric) ladder series.

In momentum space the corresponding matrices are labeled by the "spins" (including positive- and negative-energy states, frequently denoted as " ρ spin") and off-shell momenta. Discretizing the lat-

FIG. 7. Same as Fig. 1 for ϵ_3 and ϵ_4 .FIG. 8. Same as Fig. 1 for 3F_2 and 3F_3 .

ter ones, we are dealing with finite matrices. It turns out that this way of handling the BSE is superior to the iteration and summation of the Born series by ordinary Padé approximants. First, this method is less time consuming since only relatively few discretized off-shell momenta are needed to reach stability, and second, the final result is less sensitive to the accuracy of calculating the higher-order diagrams.

In applying the method to the coupled 3S_1 - 3D_1 channel, the choice of the first off-shell point is crucial for the rate of convergence of the OPA. It is most important to include from the very beginning a point $\sim \hat{p}/2$, \hat{p} being the on-shell momentum. In Table II the rate of convergence with increasing number of off-shell points is shown for the case of A coupling at 100 MeV. The off-shell points are the same as in Ref. 3, except that the order is changed in that the first off-shell point is chosen to be $\hat{p}/2$. As a result, the convergence rate is drastically improved. Similar results hold for other energies, and the final results agree very well with

TABLE II. Convergence rate and stability of OPA's with 3-10 off-shell points for A πN coupling at 100 MeV. The points are chosen as in Ref. 3. BSE gives the "exact" result obtained with the standard Padé method.

No. of points	3S_1	3D_1	ϵ_1
3	34.47	-13.90	3.19
4	38.59	-12.56	0.79
5	38.18	-12.89	1.27
6	38.58	-12.86	1.32
8	38.44	-12.91	1.26
10	38.44	-12.91	1.26
BSE	38.78	-12.88	1.30

the one obtained by applying ordinary Padé approximants to solve the BSE.

What one learns from this result clearly is that only a few off-shell momenta are important. The question arises what the number of points is which one has to choose in order to obtain reliable results. One answer to this question is to vary the off-shell momenta and investigate the stability of the result. One is thus naturally led to a variational principle, i.e., one considers the off-shell momenta as variational parameters and looks for stationary points of the phase shifts. Within the framework of the Schrödinger equation^{4,8,10} and the BSE¹¹ this method can be deduced from the Schwinger variational principle and has been applied very successfully to calculate phase shifts numerically.

In the case of the BSE with *A* coupling, we have found that an OPA with four off-shell points besides the on-shell point (in the following denoted by $[1/1]_5$) gives very accurate results for the 3S_1 phase shift. Choosing the first three points as denoted by crosses in Fig. 9, the results at 100 and 200 MeV are plotted in Figs. 10 and 11, respectively, for $\delta({}^3S_1)$ (curve *O*) as a function of the fourth off-shell point, chosen according to Fig. 9. The 3S_1 phase shift is practically constant as a function of the off-shell momentum. We have also tried out OPA's for the 3S_1 phase shift with fewer off-shell states, but, without applying a systematic search routine for finding stationary points in all off-shell momenta simultaneously, we did not find satisfactory accuracy in these cases.

IV. THE CROSSED-BOX-GRAPH CONTRIBUTION

In this section we discuss results obtained using *P* coupling for the pion. The very strong attraction found previously when we used the pseudoscalar theory for the πN interaction can mainly be ascribed to the very strong coupling between positive-

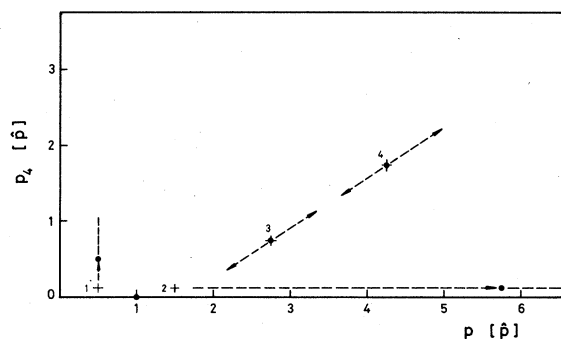


FIG. 9. Variation of the off-shell points. The four off-shell points are numbered 1-4, and their region of variation is indicated by dashed lines.

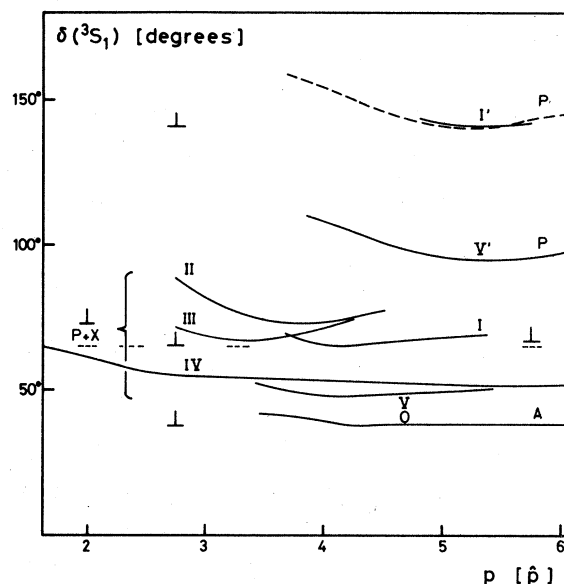


FIG. 10. The 3S_1 phase shift at 100 MeV as a function of the off-shell momenta. \perp indicates the position of point No. 3 and the height of the corresponding minimum.

and negative-energy states. One possible mechanism to weaken this coupling is to include in addition the crossed box pion-exchange graph in the calculation.

At first we investigate the cancellation between the direct and the crossed box graphs on shell. For various cutoffs our results are given in Table III for 100 MeV. Since the cancellation is expected

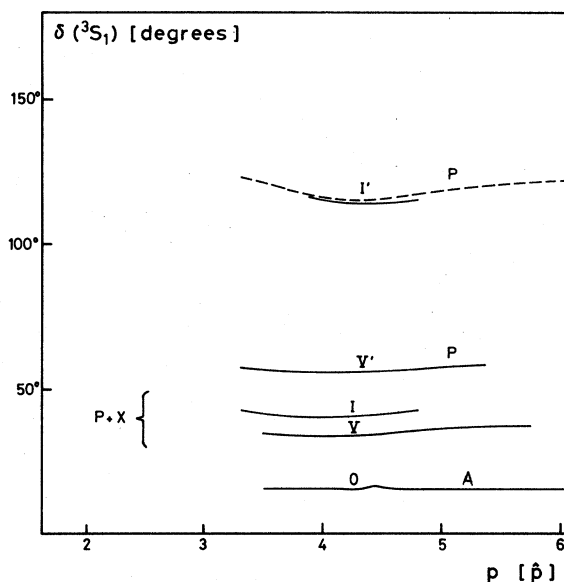


FIG. 11. Same as Fig. 11 for 200 MeV.

TABLE III. Cancellation for the on-shell K -matrix elements between the direct (D) and crossed (X) box graph for 100 MeV and various cutoffs. The result from the Blankenbecler-Sugar equation (BBS) is also shown. Only partial agreement according to Fig. 12 is obtained.

Λ^2	D			X			BBS		
	K_{11}	K_{12}	K_{22}	K_{11}	K_{12}	K_{22}	K_{11}	K_{12}	K_{22}
$1m^2$	2.85×10^{-2}	4.52×10^{-4}	-8.45×10^{-4}	-7.27×10^{-3}	9.52×10^{-5}	-4.33×10^{-5}	8.80×10^{-3}	6.86×10^{-4}	-8.69×10^{-4}
$2m^2$	4.01×10^{-2}	9.05×10^{-4}	-9.75×10^{-4}	-9.26×10^{-3}	1.40×10^{-4}	-3.48×10^{-5}	1.58×10^{-2}	1.23×10^{-3}	-9.52×10^{-4}
∞	8.56×10^{-2}	2.27×10^{-3}	-9.86×10^{-4}	-1.05×10^{-2}	3.21×10^{-4}	-2.39×10^{-5}	6.18×10^{-2}	2.75×10^{-3}	-9.23×10^{-4}

to be due to the long-range part of these graphs, it should be more significant for smaller cutoffs. This is in fact so, but the expected agreement between the second-order result with the BBS equation and the sum of crossed and direct box graphs according to Fig. 12 is not achieved. In the calculation of the crossed box graphs, the same cutoff procedure has been used as in the one-boson-exchange interaction.

The next step is to investigate the off-shell contribution of the crossed box graph. This is done in the framework of the OPA by simply adding the contribution X from the crossed box graph to D in Eq. (6). It is easily seen that this $[1/1]$ OPA is the solution of a BSE whose kernel G' is the $[1/1]$ OPA to the irreducible part,

$$G' = G(G - X)^{-1}G. \quad (7)$$

At this point it should be mentioned that when we use P coupling we have never fully succeeded in solving the ladder BSE for the 3S_1 phase shift by applying the standard method of scalar Padé approximants. The interaction apparently becomes so strong and the corresponding perturbation series so badly divergent that the ordinary Padé approximants do not converge and are extremely sensitive to the mesh used for numerical integration, i.e., to the accuracy with which the higher-order ladder graphs are calculated. Applying the $[1/1]_5$ variational OPA as before, we obtained very pronounced minima which are also stable with respect to the choice of mesh. In Figs. 10 and 11 the solid curves I' give the results at 100 and 200 MeV. Also shown are the results (dashed curves I') obtained with half the number of mesh points. From this we see that the stability is satisfactory with respect to integrations. The curves for A and P coupling in Fig. 10 show the essential difference

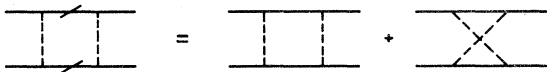


FIG. 12. Cancellation between direct and crossed box graph, to be compared with the Blankenbecler-Sugar equation (left-hand side).

that for A coupling the $[1/1]_5$ is almost a constant as a function of the off-shell momentum, while for P coupling quite a variation of the phase shift (with a minimum) is observed. From this it becomes clear that the stability of the OPA for A coupling with increasing number of off-shell points is very much due to the fact that the result is independent of the choice of the off-shell momentum, since then it is irrelevant where one puts additional points. This is not so, however, in the case of P coupling, and, in fact, even with a larger number of points no stability is reached. Therefore, we consider the variational principle as decisive, where it is understood that one has to perform variations in all off-shell momenta. One must expect that for more and larger off-shell momenta further extrema of the variational $[1/1]_n$ ($n=5, 6, \dots$) exist. In potential theory with potentials of changing sign the situation is similar. One observes in the potential case that the $[1/1]_n$ variational OPA for low n (2 or 3) gives "excellent precision at any energy and coupling strength."⁵ Since there is no particular justification for any other choice, we have to do the same in the case of the BSE, i.e., use only a few and low off-shell momenta. For the 3S_1 with A πN coupling we obtain (without a systematic multivariable search—which might improve the situation) very accurate results with four off-shell momenta. This result will be taken as a guide for the other cases. In Sec. V we demonstrate that only one off-shell momentum is necessary for higher partial waves.

Including the crossed box graph, one observes as much structure in the 3S_1 phase shift as a function of the off-shell momenta as for the P coupling discussed above. While for the A coupling it does not matter much what off-shell points have been selected, here one has to perform variation in all four off-shell momenta. Choosing the off-shell points as previously (the positions denoted by crosses in Fig. 9), we find curve I of Figs. 10 and 11. Then we have also looked for stationary points in the other off-shell momenta. The region of variations is shown in Fig. 9. We have adopted the following procedure: For other choices of point No. 3 we calculate the minimum as a function of point No. 4.

Curves II and III in Fig. 10 show these results. From this we determine the values of points 3 and 4 for which we have the lowest minimum. Subsequently, using these values we looked for a minimum as a function of point No. 2. A flat minimum is obtained at $p \sim 6\hat{p}$ (curve IV). Finally, fixing the value for point No. 2 at the minimum of this curve, point No. 1 was varied to determine the lowest minimum. The positions of the off-shell points found in this way are shown in Fig. 9 as dots. In order to see whether we can improve on this, we varied again point No. 4. As a result, we found that the minimum did not shift. This result is shown as curve V. The lowest phase shift obtained in this way is $\delta(^3S_1) = 48.0^\circ$. Finally, using this choice of off-shell points, we calculated also the phase shift when the crossed box graph is neglected. The results are shown in Figs. 10 and 11 (curve V'). From this we see that the result drops significantly as compared to the original off-shell points. However, the results are substantially larger than the corresponding results with the crossed box graph included. Taking into account that we have not performed a systematic multivariable search (i.e., not with a fitting routine) for stationary points, these numbers may come down slightly, but comparing the obtained results with the P interaction one sees that the inclusion of the crossed box graph gives rise to a weakening of the NV interaction, so that there is also a closer agreement to the results obtained with A coupling. Concerning the variations of the 3D_1 and ϵ_1 , we observe that these stay within limits of 5%. In Table IV we give a complete compilation of all results for 100 and 200 MeV.

V. VARIATIONAL OPA FOR HIGHER PARTIAL WAVES

Taking into account four off-shell points as variational parameters for the 3S_1 calculations was

TABLE IV. For 100 and 200 MeV the results for pseudoscalar (P), P including the crossed box graph ($P+X$), and axial-vector (A) coupling are presented as calculated from a $[1/1]_5$ variational OPA. The given numbers correspond to the minima in curves V', V, and O, respectively, of Figs. 10 and 11.

Energy (MeV)	Interaction	3S_1	3D_1	ϵ_1
100	P	94.5	-14.4	-1.7
	$P+X$	48.0	-14.0	3.7
	A	38.2	-12.9	1.3
200	P	56.1	-30.2	0.60
	$P+X$	34.2	-24.6	3.4
	A	15.3	-19.9	0.65

motivated by the experience with A coupling. Although three off-shell points give acceptable results in that case, the accuracy obtained with four off-shell states may be achieved only by applying a systematic fitting routine which really finds the stationary point in the six variables [$3 \times (\text{modulus of momentum} + \text{relative energy})$]. In any case quite a few off-shell points are used for the 3S_1 calculation owing to their complicated structure. To support the idea that one should use a low number of off-shell points, we demonstrate in this section what results when only one off-shell point is used as variational parameter for the higher partial waves (see also Ref. 3).

Figure 13 gives results for various partial waves at 100 MeV. There are "poles" in the phase shifts (the poles are actually poles in $\tan\delta$), but always the first minimum gives an extremely good approximation to their correct value. To remove the ambiguity of taking the minimum or maximum, one has in principle to consider their dependence on the relative energy variable p_4 . For this purpose we have calculated for the 1S_0 channel at 100 MeV and

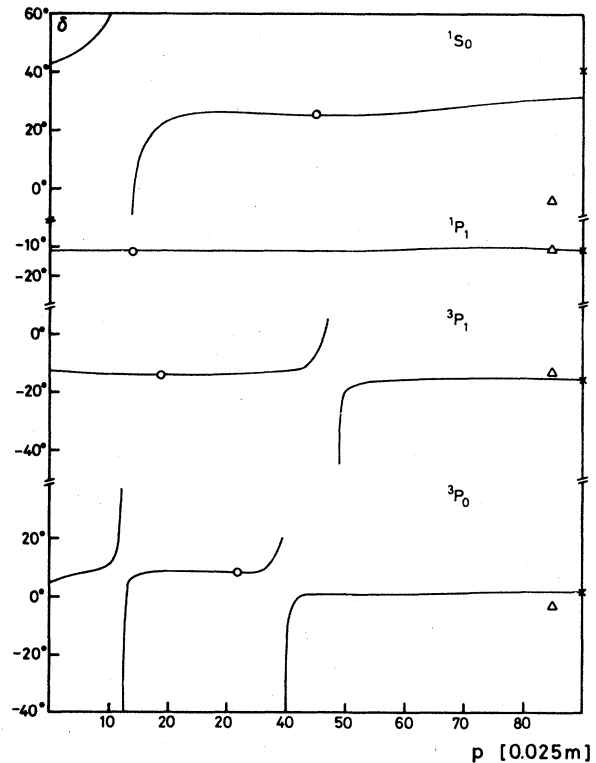


FIG. 13. $[1/1]_1$ variational OPA for A coupling and various partial waves at 100 MeV; the meaning of the symbols is: \circ = "exact" value (obtained by standard Padé's); \times = matrix Padé only on-shell momentum, but off-shell in "spin"; \triangle = scalar Padé.

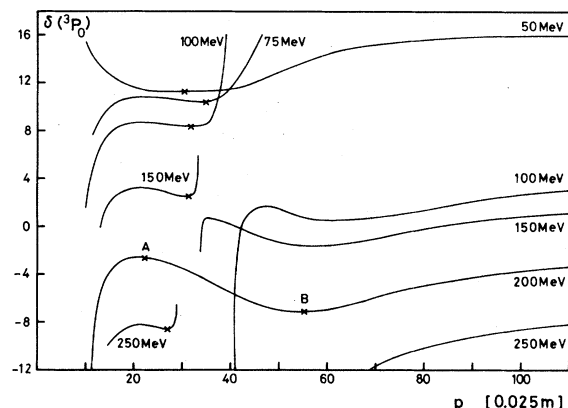


FIG. 14. $[1/1]_1$ variational OPA for 3P_0 phase shift (A) and various energies. The crosses denote the positions of the extrema.

various p values the phase shift as a function of p_4 . As a result, we find always a minimum in the p_4 variable. For a certain value of p and p_4 this minimum coincides with the first maximum in p , giving rise to a saddle point in the p - p_4 plane. The value of δ at this point is in excellent agreement with the "exact" phase shift. This suggests that one should possibly look for a saddle point in the p - p_4 plane as the proper stationary point. Another striking example is shown in Fig. 14. It shows results for the 3P_0 phase shift at various energies. Again, the first minimum gives the correct result, except for 200 MeV, in which case the first maximum is closer to the exact result. The difference with respect to the other energies is that there is no pole in p . Apparently there is a region in E , where the pole is gone as a function of p ; and, instead of having a local minimum as a function of p , one has to take a local maximum. Taking into account variations

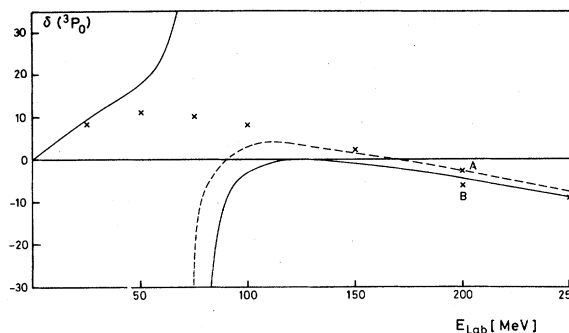


FIG. 15. 3P_0 phase shift (see Fig. 14) obtained with $[1/1]_1$ variational OPA. The figure demonstrates that the variational OPA can produce the zero of the phase shift. Full line: scalar approximant; dashed line: matrix approximant. The crosses denote the calculated values at the extrema.

in p_4 , this ambiguity can possibly be resolved as well.

Figure 15 finally shows the 3P_0 phase shift as a function of energy. It should be noted that the variational principle does in fact yield the zero of the phase shift properly, which neither the ordinary "scalar" nor "matrix" (off-shell in spin, on-shell in momentum) Padé approximant can do. This property has been observed in potential theory as well.¹⁰

ACKNOWLEDGMENT

One of us (J.F.) would like to thank the Theory Division of Saclay, in particular Prof. D. Bessis, for the warm hospitality extended to him during a visit. Calculations on the variational OPA's were performed at this time which were decisive for that part of the present work.

¹J. Fleischer and J. A. Tjon, Nucl. Phys. **B84**, 375 (1975).

²J. Fleischer and J. A. Tjon, Phys. Rev. D **15**, 2537 (1977).

³J. Fleischer and J. A. Tjon, in *Padé and Rational Approximation*, edited by E. B. Saff and R. S. Varga (Academic, London and New York, 1977).

⁴L. P. Benofy, J. L. Gammel, and P. Mery, Phys. Rev. D **13**, 3111 (1976); L. P. Benofy and J. L. Gammel, in *Padé and Rational Approximation*, edited by E. B. Saff and R. S. Varga (Academic, London and New York, 1977).

⁵D. Bessis and G. Turchetti, Nucl. Phys. **B123**, 173 (1977).

⁶K. Fabricius and J. Fleischer, Phys. Rev. D **19**, 353 (1979); K. Fabricius and J. Fleischer, in *Few Body Systems and Nuclear Forces I*, Springer Lecture Notes in Physics, Vol. 82, edited by H. Zingl, M. Haf-

tel, and H. Zankel (Springer, Berlin and New York, 1978).

⁷P. A. Verhoeven, Ph.D. thesis, Catholic University, Nijmegen, 1976 (unpublished).

⁸J. Nutall, in *The Padé Approximant in Theoretical Physics*, edited by G. A. Baker, Jr. and J. L. Gammel (Academic, London and New York, 1970).

⁹J. L. Basdevant, D. Bessis, and J. Zinn-Justin, Nuovo Cimento **60A**, 185 (1969); D. Bessis, in *Padé Approximants*, edited by P. R. Graves-Morris (Institute of Physics, London and Bristol, 1973).

¹⁰C. Alabiso, B. Butera, and G. M. Prospero, Nucl. Phys. **B31**, 141 (1971).

¹¹C. Alabiso, P. Butera, and G. M. Prospero, Nucl. Phys. **B46**, 593 (1972).

¹²M. H. Mac Gregor, R. A. Arndt, and R. M. Wright, Phys. Rev. **182**, 1214 (1969).